High temperature mechanical properties of reaction-sintered mullite/zirconia and mullite/alumina/zirconia composites

G. ORANGE, G. FANTOZZI
GEMPPM (LA 34 CRRACS), Bât. 502, INSA, 69621 Villeurbanne, France

F. CAMBIER, C. LEBLUD, M. R. ANSEAU*, A. LERICHE
CRIBC, Avenue Gouverneur Cornez, 4, 7000 Mons, Belgium

Strength and fracture toughness of reaction-sintered mullite/zirconia composites (RSMZ) and reaction-sintered mullite/alumina/zirconia composites have been investigated as a function of temperature. Thermal shock resistance has also been determined. It was found that dispersion of zirconia particles and the particular microstructure of mullite obtained by means of an *in situ* reaction process leads to improved properties, with a room temperature fracture toughness of about 5.25 MPa m$^{1/2}$. Up to 1000° C fracture strength and toughness values are quite high, which make these materials potential candidates for high temperature applications.

1. Introduction

Mullite as alumina and aluminosilicate ceramics are among the most used materials for traditional refractory applications. There is today an increasing interest in ceramic materials with improved mechanical behaviour under high temperature structural applications.

Mullite, however, despite its unique thermal properties, has not been so widely studied because of its relatively poor mechanical properties as well as difficulty in sintering. To enhance its properties, work has been devoted to different preparation routes such as hot-pressing, sol–gel processing or coprecipitation [1–3]. It has also been well-stated that incorporation of monoclinic or tetragonal zirconia particles is able to improve the strength and toughness of ceramic bodies [4–5].

There are two main processing routes for producing mullite/zirconia composites, each leading to a special microstructure and to specific properties. Mullite/zirconia composites can be produced by conventional sintering of mechanical mixtures of fused mullite [6] or active pre-mullite [7] and ZrO_2 powders (SMZ).

These composites can also be produced by *in situ* reaction processes between zircon ($ZrSiO_4$) and alumina to form mullite with dispersed ZrO_2 (RSMZ) following [8, 9]:

$$2ZrSiO_4 + 3Al_2O_3 \rightarrow 2ZrO_2 + 3Al_2O_3 \cdot 2SiO_2$$

$$(1)$$
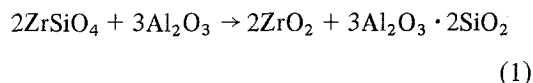
Two different reaction-sintering ways have been used in order to obtain dense composites. First, a two-stage process, separating densification and reaction [10] after attrition milling and isostatic pressing of the raw materials. In the second method additives are used in order to achieve reaction and densification simultaneously [11, 12].

The stoichiometry of Equation 1 can be easily modified as :

$$2ZrSiO_4 + (3 + x)Al_2O_3 \rightarrow 2ZrO_2$$
$$+ 3Al_2O_3 \cdot 2SiO_2 + xAl_2O_3 \qquad (2)$$
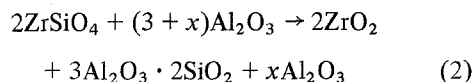
It is then possible to produce ceramic matrices containing mullite and alumina with dispersed zirconia particles leading to multiphase ceramic alloys of the zirconia/alumina/mullite type (ZAM).

*Present address: Cookson Central Research Laboratory, Wadsworth Road, London UB6 7JQ, UK.

Moreover, in such reaction-sintered materials the ZrO_2 content can be modified to a given level by substituting the fine zircon by partly dissociated zircons in which higher zirconia contents are obtainable [9].

The purpose of the present work is to check the two above mentioned ways (Reactions 1 and 2) by producing reaction-sintered mullite/alumina/zirconia ceramics in order to measure their room and high temperature mechanical properties to compare with those of reaction-sintered mullite/zirconia and other similar materials (RSMZ, SMZ).

2. Experimental procedure
2.1. Processing
Three sets of materials were prepared by reaction sintering of mixed powders, with final composition given by using an excess of alumina or dissociated zircon of various compositions.

(a) ZAM 1

Mullite/zirconia material according to Equation 1 by adding 1.8 wt % of magnesia to the mixture:
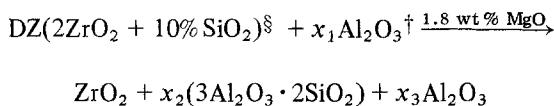
$$2ZrSiO_4{}^* + 3Al_2O^\dagger \xrightarrow{1.8\,wt\%\,MgO\ddagger}$$
$$2ZrO_2 + 3Al_2O_3 \cdot 2SiO_2$$
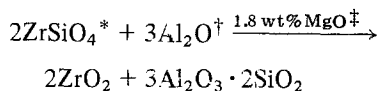
(b) ZAM 2

Mullite/alumina material according to Equation 2 by adding 1.8 wt % of magnesia to the mixture and by calculating x in order to obtain 20 vol% ZrO_2 in the prepared material:

$$2ZrSiO_4{}^* + (3+x)Al_2O_3{}^\dagger \xrightarrow{1.8\,wt\%\,MgO\ddagger}$$
$$2ZrO_2 + 3Al_2O_3 \cdot 2SiO_2 + xAl_2O_3$$
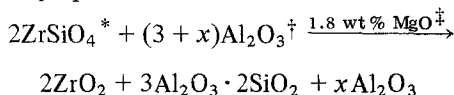
(c) ZAM 3

Alumina/mullite/zirconia material from Equation 2 with dissociated zircon (DZ) as raw material, the stoichiometry being chosen to obtain 20 vol% ZrO_2 in the prepared material:

$$DZ(2ZrO_2 + 10\% SiO_2)^\S + x_1 Al_2O_3{}^\dagger \xrightarrow{1.8\,wt\%\,MgO}$$
$$ZrO_2 + x_2(3Al_2O_3 \cdot 2SiO_2) + x_3 Al_2O_3$$

Magnesia was used as a reaction-sintering additive in each of these three sets of materials to decrease the temperature of dissociation of zircon and produce a small amount of transient

TABLE I Crystalline phase content of the materials (vol%)

ZAM 1	ZAM 2	ZAM 3
75% mullite	56% mullite	72% Al_2O_3
25% ZrO_2	26% Al_2O_3	11% mullite
	18% ZrO_2	17% ZrO_2

liquid phase contributing to the densification simultaneously with the reaction [12]. As a consequence some residual (amorphous) phase containing magnesium aluminosilicates can be found at grain boundaries in the resulting ceramic bodies.

In order to determine the sintering conditions, the powder batches ZAM 1, ZAM 2 and ZAM 3 were mixed using mechanical procedures with an organic binder. About 4 wt % of Butvar B98 (Monsanto) was dissolved in dioxan for 4 h and the resulting paste was dried and ground. The mixture obtained by uniaxial pressing (50 MPa) in a cylindrical die (20 mm diameter). After debonding, the samples were reaction sintered in air between 1450 and 1650° C for 15, 30, 60 and 120 min. The porosity of each sample was measured by liquid displacement and the content of tetragonal zirconia was determined by the Garvie–Nickolson method. Optimal reaction-sintering conditions have been determined by biaxial flexure strength of discs (26 mm diameter, 4 mm thickness) tested at a constant loading rate of 30 N sec^{-1} [13].

Samples have been specially prepared for the determination of the mechanical behaviour (fracture strength and toughness) by mixing powders in water 4 wt % PEG¶ and spray drying the slip.

The granules were compacted by uniaxial pressing (50 MPa) in the shape of parallelepipeds (150 mm × 25 mm × 25 mm). After debonding the bars were reaction sintered using the best temperature and time conditions determined by the previous mechanical tests. Reaction sintering was carried out at respectively 1500° C for 15 min (ZAM 1), 1500° C for 30 min (ZAM 2), 1500° C for 2 h (ZAM 3).

Phase composition of the three materials are listed in Table I.

2.2. Mechanical properties
The mechanical behaviour of the three sets of RS

---

*Opazir S (Quiminsa, Spain). Specific area, 5.4 m^2 g^{-1}; average grain size, 1.35 μm.

$\dagger$80% RC172DBM–20% RC152DBM (Reynolds Chemicals, USA).

$\ddagger$Mag. Chem. 10 (Martin Marietta, USA). Specific area, 0.45 m^2 g^{-1}.

$\S$DZ Zedox 5 (Anzon Ltd, UK).

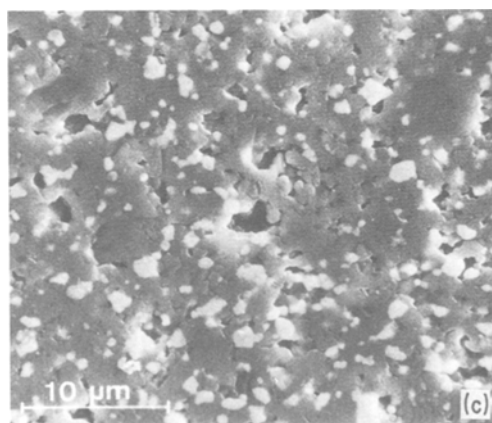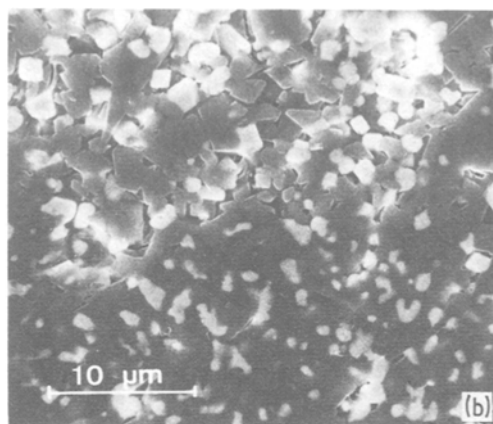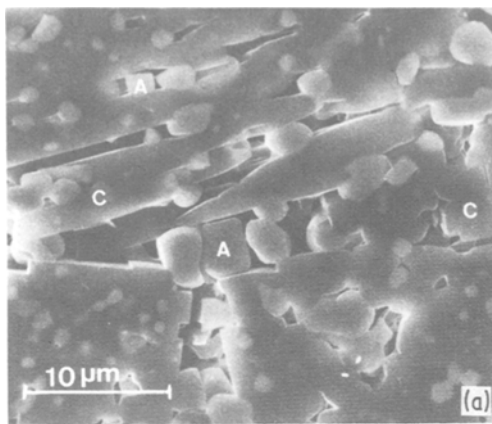$\P$ Polyethylene glycol, MM4000, Hoechst, Germany.

Figure 1 SEM micrographs of 3 composites. (a) Polished surface after chemical etching of ZAM 1. (b) Polished surface after chemical etching of ZAM 2. (c) Polished surface after thermal etching of ZAM 3.

mullite zirconia and mullite/alumina/zirconia composites has been studied at room temperature and up to 1200°C, in air, using bending tests [14].

The strength measurements have been made on specimens of rectangular section (6 mm × 3.5 mm) using three-point bending with a span of 21 mm. Flexural strength (σ_F), yield stress (σ_e) and elastic modulus (E) can be deduced from the measured values of load and deformation.

The fracture toughness, K_{IC}, has been calculated from fracture values obtained with single-edge notched beam (SENB) tested in three-point bending. Specimens were notched (diamond saw of 100 μm width) to a relative depth (a/w) of about 0.4 and tested in the "as diamond machined" condition. No effect on mechanical properties has been detected after short time annealing treatments (1100 to 1400°C). This point has been observed by Wallace et al. [15] also on similar RS materials, and has been correlated to the absence or stability of surface compressive stresses.

All measurements have been carried out in air, at a constant cross-head speed of 0.1 mm min^{-1} (strain rate: $\dot{\epsilon} \sim 8 \times 10^{-5}$ sec^{-1}).

Thermal shock resistance has been determined by flexural strength measurement after quenching in cold water from different temperatures.

3. Results
3.1. Microstructure

The obtained microstructures are specific to the reaction sintering process. The use of MgO additions involves the formation of a liquid phase during the process and promotes the dissociation of zircon in ZAM 1 and ZAM 2. The examination of the quaternary MgO–SiO$_2$–Al$_2$O$_3$–ZrO$_2$ phase diagram shows that for the two studied compositions the first phase which crystallizes is zirconia and the second one is mullite, with as a consequence the embedding of a large proportion of zirconia particles in the mullite grains.

These intragranular zirconia particles are more numerous in ZAM 1 than in ZAM 2 due to the higher zircon content in the raw ZAM 1 material. In the same way the lower silica content in ZAM 3 leads to a lower liquid phase volume. The ZAM 3 microstructure is then close to alumina zirconia composites obtained by milling followed by sintering.

Typical microstructures respectively of ZAM 1, 2 and 3 are presented in Figs. 1a, b and c (polished surfaces after chemical etching for ZAM 1 and ZAM 2 and after thermal etching for ZAM 3). The microstructure of ZAM 1 material is always constituted by elongated and crosslinked grains of mullite.

The chemical etching does not reveal the grain

2535

TABLE II Room temperature fracture characteristics

| | ZAM 1 | ZAM 2 | ZAM 3 | Mullite | | RSMZ | SMZ | SMZ | Al$_2$O$_3$ | |
				HP	Sintered				Sintered	HP
σ_F (MPa)	270 ± 20	315 ± 20	330 ± 20	270	150	425	200 500 after HIP	290	300	610
K_{IC} (MPa m$^{1/2}$))	4.6 ± 0.2	4.75 ± 0.2	5.25 ± 0.2	1.8		4	3.5	3.1	3	4.9
ΔT (°C)	360	325	285	300		–	–	–	200	
	This work			[16]		[10–17]	[6–17]	[18]		[19]

NB All composites contain 20 vol % ZrO$_2$.

boundaries between the different mullite grains (these boundaries can be revealed by thermal etching), showing that no liquid phase is present along them.

Glassy phase is contained in the tridimensional skeleton of mullite. Two types of zirconia particles can be observed: rounded intragranular (C) and well-faceted intergranular (A). A particles are much larger than C ones (average size about 2.5 μm for A and less than 1.0 μm for C). In the ZAM 2 materials, mullite grains are less elongated as shown in Fig. 1b.

3.2. Mechanical behaviour
3.2.1. At room temperature
The material characteristics, fracture toughness, strength and thermal shock resistance are listed in Table II and compared with other available data.

If we consider pure mullite and alumina data, fracture properties, especially fracture toughness, of mullite/zirconia composites are enhanced. The studied material characteristics are similar to those reported by Wallace *et al.* on RSMZ prepared by two-stage processing [10, 17]. Sintered materials (SMZ) obtained from mixtures of mullite and zirconia powders have lower fracture values [6, 17, 18]. From ZAM 1 to ZAM 3 we observe a slight increase of toughness as the mullite content decreases. Thermal shock resistance is determined by the critical quenching temperature (T_c) which leads to severe cracking of the materials and so to low strength values. The thermal shock resistance of the three sets of material studied is reported in Fig. 2.

ZAM 1, which is composed of mullite and dispersed ZrO$_2$ particles, shows a better thermal shock resistance than other ZAM materials and even than pure mullite (see Table I).

3.2.2. At high temperature
Values of flexural strength (σ_F) and critical stress intensity factor (K_{IC}) at the various temperatures (up to 1200° C) are presented in Figs. 3 and 4. Pictures of fracture faces are presented:
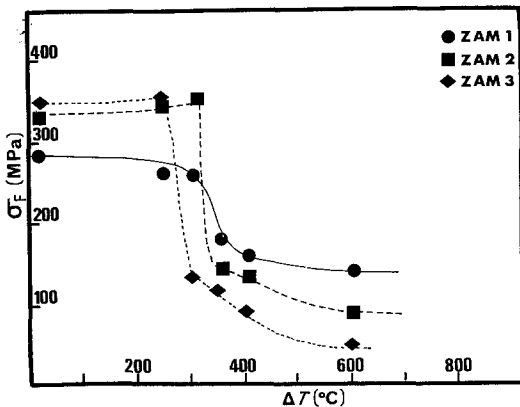

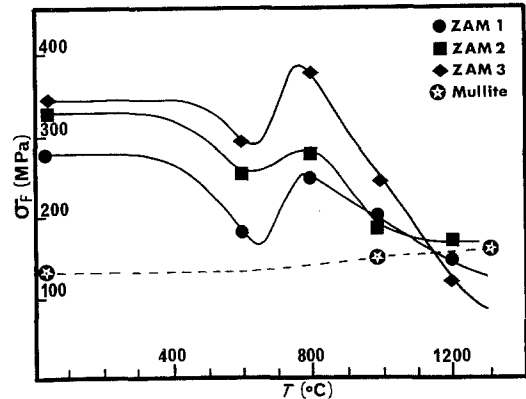*Figure 2* Flexural strength of ZAM materials after quenching from different temperatures.

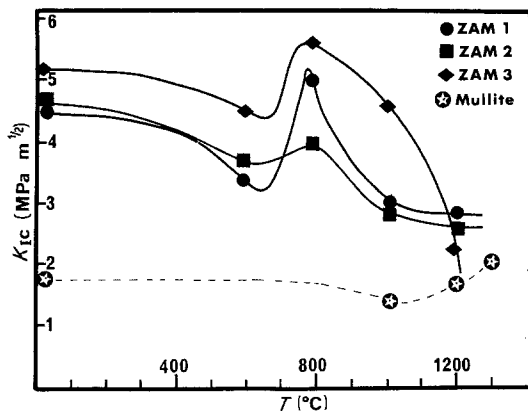*Figure 3* Temperature dependence of the modulus of rupture, σ_F.

Figure 4 Temperature dependence of the fracture toughness, K_{IC}.

At room temperature: Figs. 5a, b and c (ZAM 1, 2, and 3)

At 1000°C: Figs 6a and b (ZAM 1), and 7a, b and c (ZAM 1, 2 and 3)

At high temperature, the three sets of material show a similar behaviour. From room temperature to 600°C there is a slow and continuous decrease of bend strength and fracture toughness. Between 600 and 800°C, the characteristics increase then fall down above 800°C.
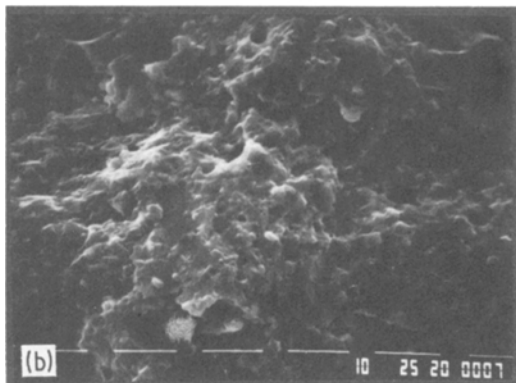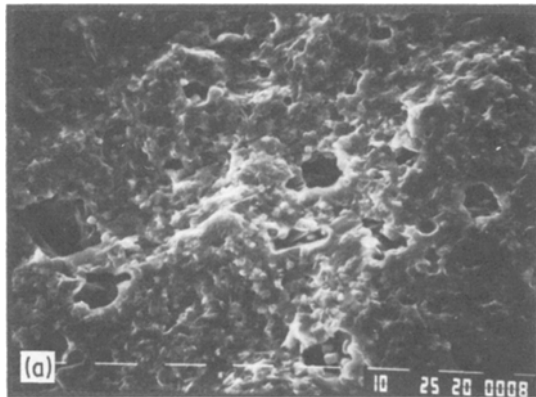
No plasticity or nonlinear behaviour was observed in bend tests, except for ZAM 3 at 1200°C.

4. Discussion

The fracture behaviour (fracture strength) is mainly controlled by internal flaws, the critical values (a_c) calculated from experimental data being about 100 to 150 μm: $\sigma_F = K_{IC}/Y(a_c)^{1/2}$. This has been confirmed by SEM observations of fracture faces. Such defects could probably result from heterogeneities in the raw materials mixture [20]. So higher fracture strength values could be reached by a better control of starting mixtures.

Differences in mechanical behaviour between the three composites (ZAM 1, ZAM 2 and ZAM 3) can be correlated both to the compositions and the particular microstructure of each set.

4.1. Low temperature behaviour (up to 600°C)

When considering the mechanical behaviour at room temperature and up to 600°C, it appears that the fracture process is the same, i.e. rupture occurs by unstable crack extension from critical flaws. The mechanical properties (σ_F and K_{IC}) decrease slowly as the temperature decreases according to the reduction of fracture energy.

In order to determine the mechanisms which are responsible for the toughness values observed in these composites, we have to take into account at least two effects: a microstructure effect and zirconia toughening.

Figure 5 SEM micrographs of room temperature fracture faces for 3 sets of composites. (a) ZAM 1. (b) ZAM 2. (c) ZAM 3. Scale bar = 10 μm.
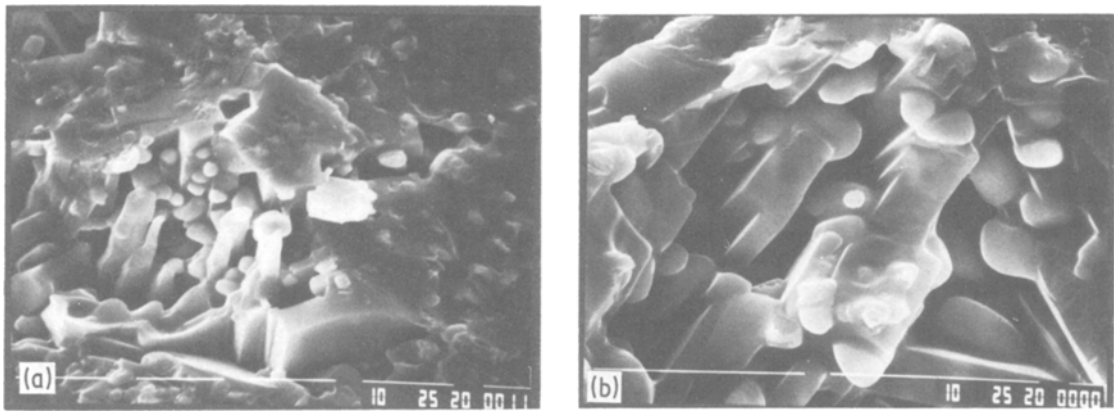

2537
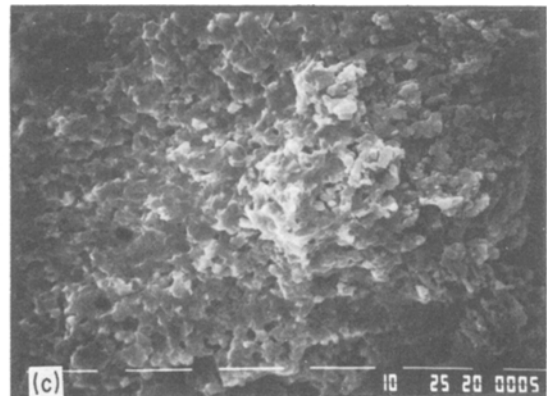
Figure 6 SEM micrographs of high temperature fracture faces after chemical etching of ZAM 1.

4.1.1. Microstructure effect

The needle-like morphology of mullite grains (Figs. 4a, 6a and b) leads to a lengthening of the fracture path and a higher proportion of transgranular fracture mode. This leads to an increase of the fracture energy. Such an effect has been observed in hot-pressed silicon nitride (HPSN) where the fracture toughness, K_{IC}, values can be increased by optimization of the microstructure related to the $\alpha-$ to $\beta-Si_3N_4$ ratio [21].

In the ZAM 2 and ZAM 3 materials, this needle-like microstructure does not appear as clearly as in ZAM 1 and the toughness increase compared to classical mullite and alumina cannot be explained by such considerations.

4.1.2. Zirconia toughening

The other factor is a toughening effect induced by zirconia particles. It has not been established which mechanism is the dominant one, transformation toughening, microcracking or some other. Most experiments were carried out with zirconia volume almost constant, determined by the reaction-sintering conditions, and so no correlation has been established with the volume fraction of zirconia particles.

Transformation toughening has not been demonstrated as an effective mechanism. Some facts do not agree with this interpretation:
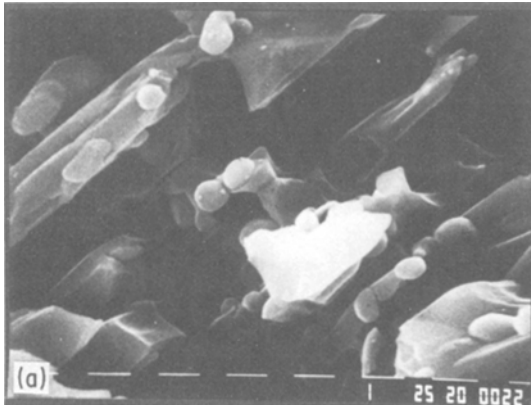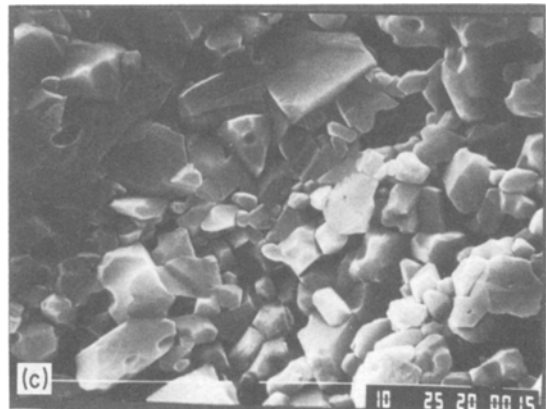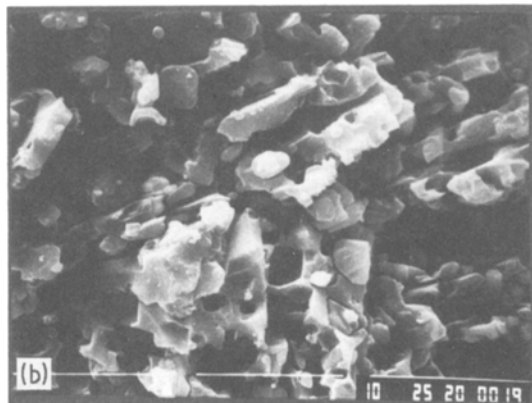

Figure 7 SEM micrographs of high temperature fracture faces after chemical etching. (a) ZAM 1, scale bar = 1 μm. (b) ZAM 2. (c) ZAM 3, scale bar = 10 μm.

(a) The rounded morphology of very fine intragranular zirconia grain with as a consequence less nuclei density [11, 22, 23].

(b) The stabilization of tetragonal zirconia particles by MgO, Al_2O_3 (or SiO_2) solid solution formation [24] leading to a decrease of the work of transformation.

(c) The thermal mismatch between mullite and zirconia suggest that the chemical stabilization could be more important than stress stabilization.

(d) No influence of annealing treatments on mechanical characteristics which means there are no surface stresses.

(e) K_{IC} values are nearly constant (up to 600° C) with temperature, or increase (600 to 800° C), whereas the transformation work decreases.

It has also not been demonstrated that microcracking is a predominant toughening mechanism in mullite/zirconia composites. In such a case, toughness values must be increased with the proportion of zirconia particles leading to microcrack formation [25]. However, microcracking might be considerably diminished by crack healing as the temperature increases because of the presence of a glassy phase.

Deflection toughening resulting from the presence of dispersed zirconia particles is another mechanism which has to be considered [26, 27]. Moreover, this third mechanism is not so temperature dependent as the two others.

In fact, it is more probable that the toughening effect observed in these composites is the result of a combination of different mechanisms each of them being more or less effective according to the composition and microstructure (ZAM 1 to ZAM 3).

4.2. High temperature behaviour
The increase of the fracture toughness between 600 and 800° C, which is more important for ZAM 1 and ZAM 3 than for ZAM 2, has been also observed in other ceramics (e.g. Si_3N_4 and Al_2O_3) which contain a large amount of glassy phase. The variation of K_{IC} can be correlated to the increase of fracture energy due to a reduction of crack tip stress intensity in the palstic zone ahead of the crack, by energy dissipation through relaxation occurring in the grain boundary phase. Microstructures impede important grain boundary sliding, and consequently no plasticity is observed and there is no degradation of the fracture strength (the evolution of σ_F is correlated to the increase

of K_{IC}). Differences between ZAM 1, 2 and 3 could be explained by differences in volume (and viscosity) of the grain boundary phases, the glass transition temperature (T_g) being in that range (600 to 800° C).

Above 800° C the glassy phase becomes more fluid ($T > T_g$), grain boundary sliding becomes more important than plastic relaxation and can lead to formation of crack and decohesion of the matrix leading to the decrease of mechanical characteristics.

At 1200° C some plasticity on load displacement curves for the ZAM 3 composition can be observed. The only high temperature data reported in literature are those given by Claussen and Jahn [10] relative to a reaction-sintered material (RSMZ) which retains its strength, about 330 MPa, up to 1250° C. This material has been obtained without any additives and so there is no important residual phase along grain boundaries as occurs with ZAM materials processed using MgO as an additive. Utilization of other additives could lead to an increase of refractoriness of residual phase and consequently better high temperature properties.

5. Conclusion
The mechanical behaviour of reaction-sintered mullite/zirconia composites (RSMZ) has been investigated at room temperature and up to 1200° C. It is well established that fully dense fine-grain mullite/zirconia or mullite/alumina/zirconia composites with enhanced mechanical properties can be produced by reaction-sintering routes. These materials, obtained with a low cost process (as regard to raw materials and reaction-sintering conditions) have potential uses as structural ceramics up to at least 1000° C.

It appears that published toughening mechanisms cannot explain by themselves the mechanical properties of these composites. This critical point requires further investigation in order to obtain a better knowledge of toughening in these materials, especially in mullite/zirconia, and as a consequence to improve their properties (at room temperature as at high temperature).

References
1. K. S. MAZDIYASNI and L. M. BROWN, *J. Amer.*

Ceram. Soc. **55** (1972) 548.

2. B. E. YOLDAS, *Amer. Ceram. Soc. Bull.* **59** (1980) 479.

3. B. METCALFE and J. M. SANT, *Trans. J. Brit. Ceram. Soc.* **74** (1975) 193.

4. "First International Conference on the Science and Technology of Zirconia Advances in Ceramics", Vol. 3, edited by American Ceramic Society (1981) pp. 98, 1370.

5. "Second International Conference on the Science and Technology of Zirconia, 'Zirconia 83' ", Stuttgart, June 1983, to be published in "Advances in Ceramics".

6. S. PROCHAZKA, J. S. WALLACE and N. CLAUSSEN, *J. Amer. Ceram. Soc.* **66** (1983) C-125.

7. J. S. MOYA and M. I. OSENDI, *J. Mater. Sci. Lett.* **2** (1983) 599.

8. E. DI RUPO, E. GILBART, T. G. CARRUTHERS and R. J. BROOK, *J. Mater. Sci.* **14** (1979) 705.

9. M. R. ANSEAU, C. LEBLUD and F. CAMBIER, *J. Mater. Sci. Lett.* **2** (1983) 366.

10. N. CLAUSSEN and J. JAHN, *J. Amer. Ceram. Soc.* **63** (1980) 228.

11. A. LERICHE, L. DAPRA, M. R. ANSEAU, C. LEBLUD and F. CAMBIER, Second Irish Durability and Fracture Conference, Limerick, March 1984, "Mechanically, Chemically and Thermally Induced Failure in Engineering Materials", edited by J. Bolton and S. Hampshire (NIHE, Limerick College, 1985).

12. P. PENA, J. S. MOYA, S. DE AZA, E. CARDINAL, F. CAMBIER, C. LEBLUND and M. R. ANSEAU, *J. Mater. Sci. Lett.* **2** (1983) 772.

13. ASTM "Standard Test Method for Biaxial Flexural Strength of Ceramic Substrates", ASTM F394-78 (1978).

14. G. ORANGE, thesis docteur-ingénieur, University of Lyon, June 1980.

15. J. S. WALLACE, G. PETZOW and N. CLAUSSEN, Second International Conference on the Science and Technology of Zirconia, "Zirconia 83", Stuttgart (June 1983). To be published in "Advances in Ceramics".

16. T. MAH and K. S. MAZDIYASNI, *J. Amer. Ceram. Soc.* **66** (1983) 699.

17. J. S. WALLACE, N. CLAUSSEN and S. PROCHAZKA, "Symposium on Ceramic Engine Components" October 1983, Hakone, Japan, edited by S. Sōmiya, E. Kanai and K. Ando (KTK, Tokyo, 1984) p. 642.

18. J. S. MOYA, M. I. OSENDI and J. S. WALLACE, "Zirconia 83", Stuttgart (June 1983).

19. G. ORANGE and P. HOMERIN, private communication.

20. C. BAUDIN DE LA LASTRA, P. PILATE, A. LERICHE and F. CAMBIER, *J. Trans. Brit. Ceram. Soc.* **83** (1984) 196.

21. F. F. LANGE, *J. Amer. Ceram. Soc.* **62** (1979) 428.

22. A. H. HEUER, N. CLAUSSEN, W. M. KRIVEN and M. RÜHLE, *ibid.* **65** (1982) 642.

23. M. RÜHLE and W. M. KRIVEN, *Ber. Bunsenges. Phys. Chem.* **87** (1983) 222.

24. J. S. WALLACE, PhD thesis, Universität Stuttgart und MPI (1983).

25. W. KREHER and W. POMPE, *J. Mater. Sci.* **16** (1981) 694.

26. K. FABER and A. G. EVANS, *Acta Metall. Part I* **31** (1983) 565.

27. *Idem, Acta. Metall. Part II* **31** (1983) 577.